

NASA TECHNICAL NOTE



NASA TN D-3881

01

NASA TN D-3881

LOAN COPY: RETL  
AFWL (WLIL)  
KIRTLAND AFB, TX

0130605



TECH LIBRARY KAFB, NM

# INLET SENSITIVITY STUDY FOR A SUPERSONIC TRANSPORT

*by Robert W. Koenig*  
*Lewis Research Center*  
*Cleveland, Ohio*





INLET SENSITIVITY STUDY FOR A SUPERSONIC TRANSPORT

By Robert W. Koenig

Lewis Research Center  
Cleveland, Ohio

NATIONAL AERONAUTICS AND SPACE ADMINISTRATION

---

For sale by the Clearinghouse for Federal Scientific and Technical Information  
Springfield, Virginia 22151 - CFSTI price \$3.00

# INLET SENSITIVITY STUDY FOR A SUPERSONIC TRANSPORT

by Robert W. Koenig

Lewis Research Center

## SUMMARY

This report presents a means of comparing inlet performance and weight compromises. It shows values of inlet drag coefficients and pressure recovery as a function of Mach number. These values are systematically varied from reference inlet values. It compares the effect of these changes on the basis of payload and passenger carrying capability of a fixed-ramp gross-weight supersonic transport. The transport uses four afterburning turbojet engines to fly analytically a 3500 nautical mile mission.

The inlet parameters examined are cowl-lip and nacelle-wave drag, boundary-layer bleed drag, inlet-total-pressure recovery, skin-friction drag, transonic excess-flow drag, and inlet weight.

This report includes an example that shows assumed inlet drag and weight parameters for five inlet types. It compares the changes in inlet parameters to a reference inlet. It then relates these changes to passenger carrying capability of the supersonic transport, and it compares the inlets on this basis.

## INTRODUCTION

A high-performance engine capable of efficient operation over a wide range of subsonic and supersonic speeds is required for the supersonic transport. Since the overall performance of the propulsion system is strongly affected by the performance of the inlet, the inlet design becomes an important factor in the overall analysis of the aircraft. A great deal of analytical and experimental research has been done on various supersonic inlets. References 1 to 3 discuss different inlet types, flow stability, pressure recovery, drag, and weight characteristics.

Inlet types are classified into three groups depending on where the supersonic diffusion takes place. The groups are external-compression, mixed-compression, and internal-compression inlets. Each type of inlet has certain drag, performance, and operating characteristics. One type of inlet will have high drag and good performance

while another inlet will have low drag and poor performance. Thus, some more inclusive figure of merit than inlet drag or performance is required to permit a comparison and selection of an inlet that will offer the best compromise design. As an aid in the evaluation and selection of inlets, this report presents data showing how variations in the basic inlet parameters are reflected in an overall airplane criterion, namely, the number of passengers, or payload. Data are given for a representative supersonic-transport airplane (fixed arrow-wing airframe; Mach 3 cruise; with afterburning turbojet; 3500-nautical-mile range, ramp gross weight, 480 000-lb) with the belief that the relative effect of inlet parameters will be about the same for other engine-airplane types.

An example is included that shows the assumed inlet drag and weight parameters for five inlet types in order to illustrate how variations in the inlet parameters that were studied affect the number of passengers of the supersonic transport when related to a reference inlet. The parameters and their respective range for this study are as follows: (1) inlet-total-pressure recovery was varied from 0.70 to 0.95 at Mach 3, (2) excess-flow drag coefficient ranged from 0.12 to 0.24 at Mach 1.2, (3) bleed drag coefficient was changed from 0 to 0.07 at Mach 3, (4) cowl-lip-wave drag coefficient was changed from 0 to 0.10 at supersonic speeds, (5) nacelle-wave drag coefficient was changed from 0 to 0.10, (6) inlet-nacelle skin-friction drag coefficient was varied from 0.035 to 0.055 at Mach 3, and (7) inlet weight was changed  $\pm 60$  percent.

## METHOD OF ANALYSIS

### Mission

The aircraft considered were designed for Mach 3 cruise with a total range of 3500 nautical miles. The flight path with respect to Mach number and altitude was fixed up to Mach 1. At higher Mach numbers, all the aircraft did not fly the same flight path. The altitude was allowed to increase as necessary to avoid the sonic-boom overpressures in excess of 2.0 pounds per square foot on the ground even though they all had the same 480 000 pounds ramp gross weight. The instantaneous weight on reaching the sonic threshold and fuselage size affect the sonic-boom overpressure; therefore, the flight path varied from one case to another. On completion of the climb phase, cruise began at the altitude which maximized the Breguet cruise factor. During cruise, altitude increased so that the Breguet factor was maintained constant at its maximum value. This resulted in minimum fuel consumption during the cruise phase of the flight. Letdown commenced at a range of 3100 nautical miles. A standard flight plan for the fixed arrow-wing airplane in altitude and distance coordinates is presented in figure 1 and is used throughout the report as the reference mission.

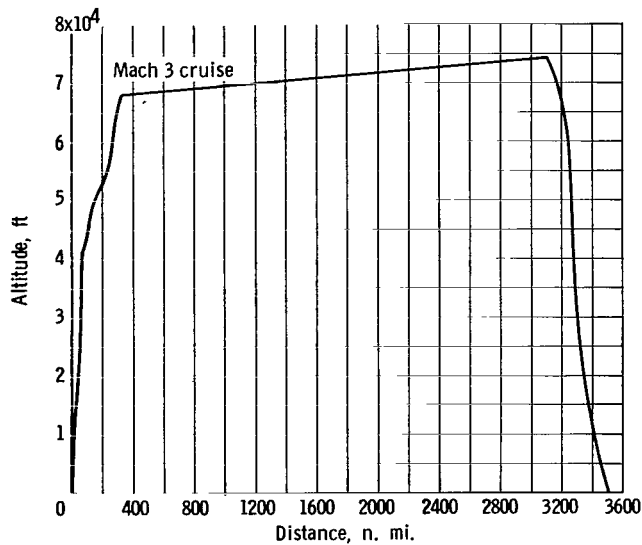


Figure 1. - Standard mission profile. Fuel reserves for (1) 7 percent of total mission fuel, (2) extension of 261 nautical miles at Mach 3, and (3) 30 minute hold at Mach 0.6.

The fuel reserve for the mission is sufficient to allow for (1) an additional 7 percent of the total mission fuel, (2) an extension of 261 nautical miles to an alternate airport at cruise altitude and Mach number, and (3) a 30-minute hold at 15 000 feet altitude at Mach 0.6. An additional fuel allowance was incorporated in the mission fuel for a 25-minute idle prior to takeoff as well as 1 minute of maximum augmentation power application prior to takeoff roll. To simplify the calculations, it was assumed that the descent time and range remained constant for all cases at 25 minutes and 400 nautical miles, respectively, with fuel consumption calculated with engines idling.

## Airframe

The aerodynamics used for this study were based on wind-tunnel data supplied by NASA Langley Research Center for the SCAT 15F, an advanced fixed-sweep arrow-wing supersonic-transport configuration similar to the one shown in figure 2.

Changes in the various inlet parameters resulted in a change in number of passengers. The fuselage was allowed to lengthen or shorten to accommodate more or less passengers. Appropriate structural weight and drag penalties or benefits are accounted for with payload variations. The fuselage weight was assumed to vary with length according to the curve presented in figure 3 (from ref. 4). The fuselage-weight term does not include the weight of passenger furnishings and services, emergency equipment,

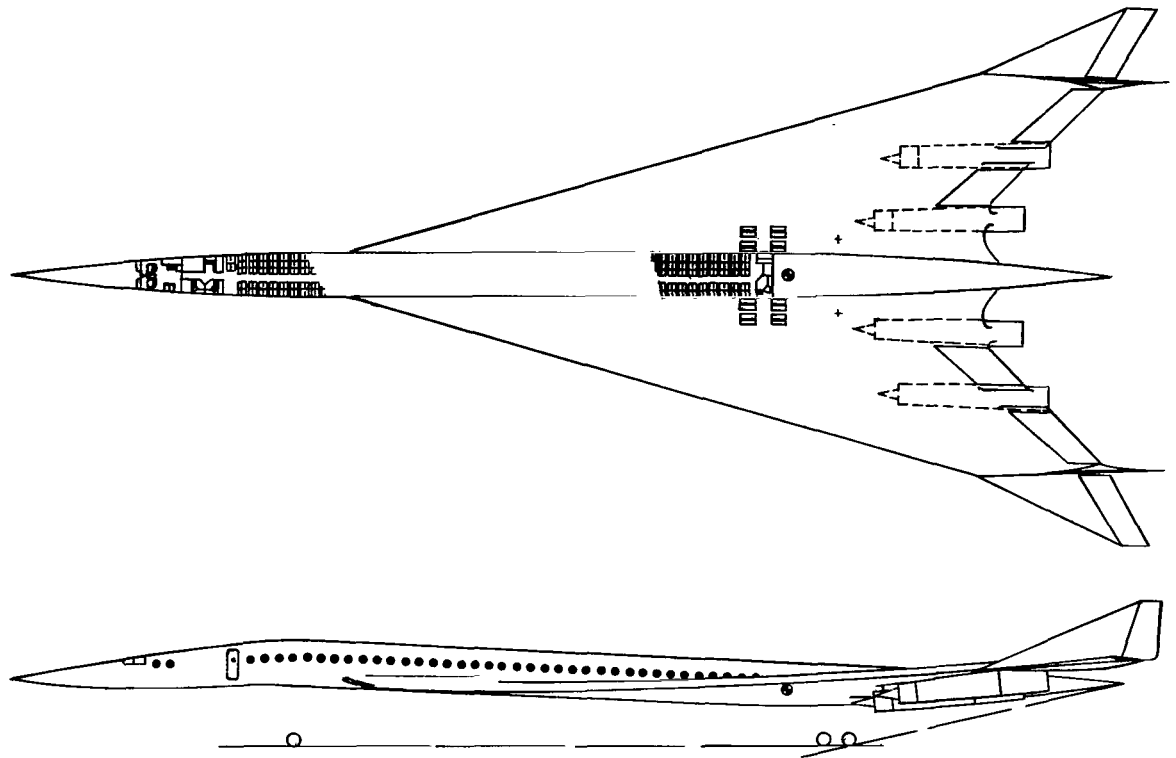


Figure 2. - Typical supersonic transport configuration.

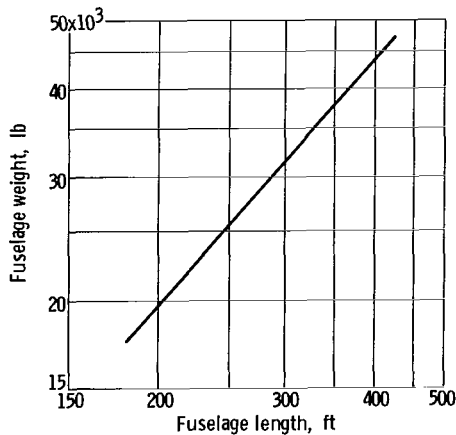


Figure 3. - Variation of fuselage weight with length (from ref. 4).

air conditioning, etc., all of which are functions of the passengers aboard. In this analysis, each additional passenger was considered to require 116 pounds of furnishings and other equipment plus 200 pounds for the passenger and baggage.

The form of the Langley aerodynamic data was modified in order to evaluate the effect of changes in fuselage length. The associated change in airplane drag was assumed to be equal to the net change in skin-friction drag of the fuselage when viewed as an isolated element. However, the effect on the total airplane drag was nearly negligible.

A representative value of the Mach 3 cruise lift to drag ratio for a typical configuration would be 9.2. The drag incorporated into this ratio is the total drag and includes engine drag. The airframe is carefully designed and area ruled to minimize the drag and sonic-boom overpressure profile.

## Engines

A single-spool afterburning turbojet with a design compressor pressure ratio of 10 and a turbine inlet temperature of  $2100^{\circ}$  F was the engine used throughout the investigation. Studies in reference 5 indicate that this pressure ratio would be nearly optimum for this turbine-inlet temperature. The maximum afterburner temperature in all cases was  $3000^{\circ}$  F. Takeoff was at the maximum dry, or unaugmented, power setting. The noise level was calculated to be 119 perceived noise decibels (PNdB) at a distance of 1500 feet from the centerline of the runway at the start of takeoff roll, when the effects of engine shielding and ground attenuation are considered. Afterburning was not used during takeoff because the noise produced by the maximum unaugmented power setting was deemed to be the maximum acceptable level of airport noise. Afterburning was initiated at an altitude of 36 000 feet where the transonic threshold is encountered and wave-drag increases rapidly. Afterburner gas temperature remained at  $3000^{\circ}$  F until Mach 2.8, at which point it was gradually reduced to  $2540^{\circ}$  F at Mach 3 and 60 000 feet altitude prior to entering the cruise mode of operation. Without this afterburner gas-temperature reduction beginning at Mach 2.8, excessive thrust minus drag margins would have resulted during climb, thus creating computational difficulties when the equations of motion are integrated. The afterburner temperature during cruise was determined by maximizing the Breguet factor.

In calculating the engine design and off-design performance, the engine components were matched to satisfy the relations involving continuity of flow, engine rotational speed, and power balance between the compressor and its driving turbine. When the engine performance was calculated, the total installation drag was taken into account as a thrust degradation of the engine. The nozzle considered for the turbojet engine was a variable geometry convergent-divergent ejector type. The nozzle thrust coefficient, which was adjusted to incorporate nozzle boat-tail drag, was included in the performance calculations as a function both of free-stream Mach number and engine power setting. "Installed-engine performance" refers to the engine performance that has been adjusted to include thrust degradation resulting from total installation drag, internal nozzle performance, and external boat-tail drag. The total installation drag is the drag of the inlet-nacelle combination based on an isolated engine concept.

## Reference Inlet

The effect of inlet parameters will generally be shown in terms of perturbations from the performance of a reference inlet. A typical mixed-compression inlet-nacelle

combination and the drags investigated are shown for an afterburning turbojet engine in figure 4. The inlet is assumed to be an axisymmetric inlet with a translating centerbody for engine-airflow scheduling. This type of inlet has an estimated inlet-total-pressure recovery at the compressor face for changing flight Mach numbers as shown on figure 5. This pressure-recovery schedule in conjunction with the typical supersonic-turbojet engine-airflow schedule (fig. 6) is used to calculate the inlet capture area and the various inlet drag coefficients when the inlet and engine are assumed to be operating at free-stream flight Mach number conditions. A method for estimating the various drag coefficients is discussed in the appendix.

Figure 7 shows the drag coefficients as a function of free-stream flight Mach number of the inlet used for the reference case. The sensitivity of payload to variations of these coefficients was determined. However, the placement of the inlet nacelle and engines on the supersonic transport is such that they will operate in the shock field of the wing,

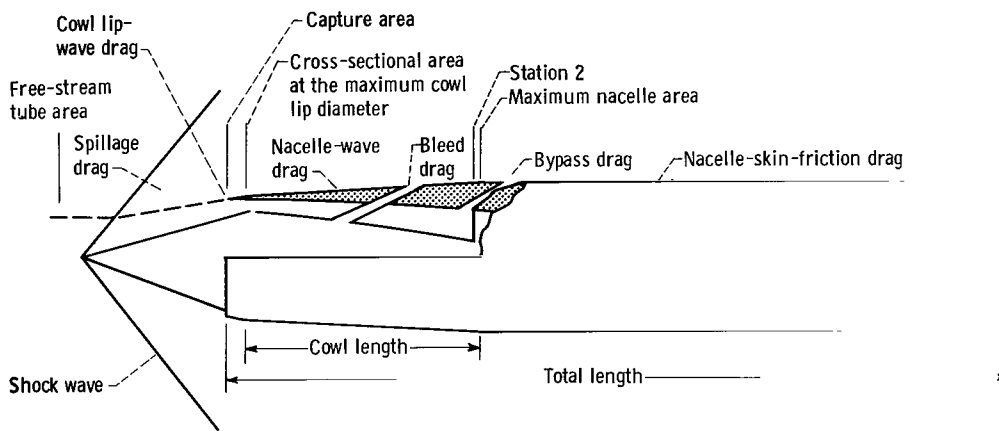


Figure 4. - Schematic drawing for inlet-nacelle reference configuration.

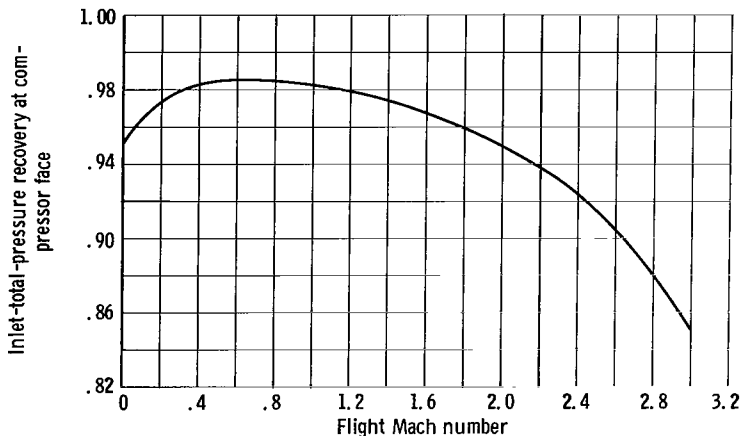


Figure 5. - Reference-inlet-pressure recovery at free-stream flight Mach number.

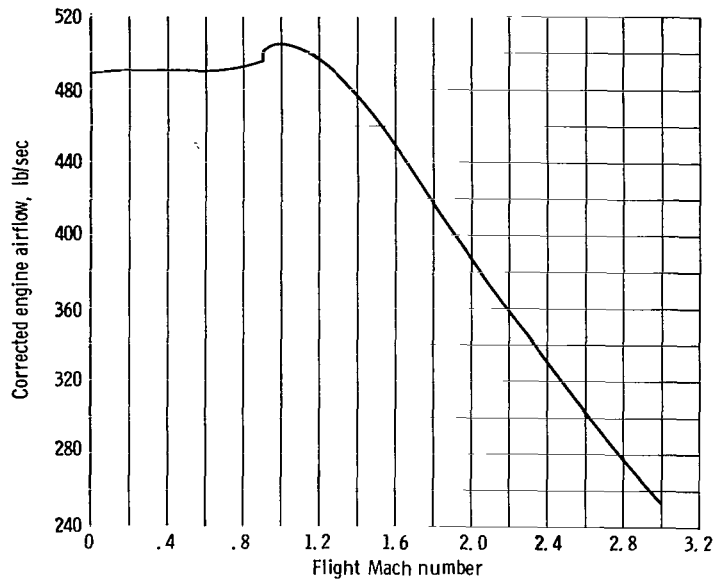


Figure 6. - Afterburning turbojet corrected engine airflow. Maximum design turbine-inlet temperature, 2100° F; design compressor pressure ratio, 10.

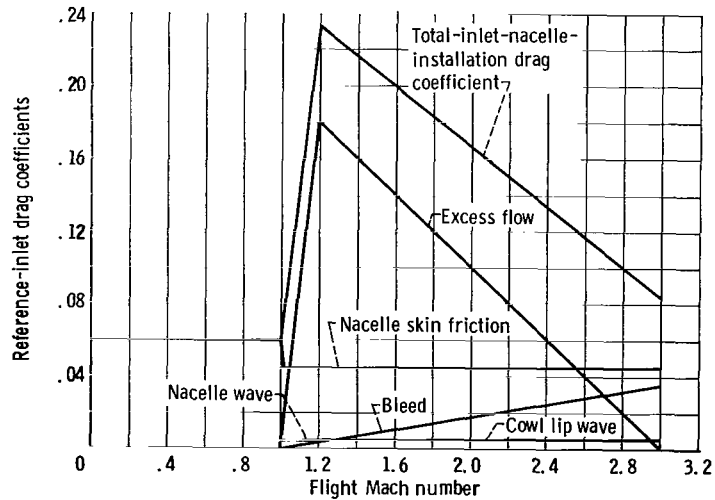


Figure 7. - Drag characteristics of reference inlet based on inlet capture area at Mach 3. Total drag coefficient equal to excess-flow plus nacelle-skin-friction plus nacelle-wave plus cowl-lip-wave plus bleed drag coefficients.

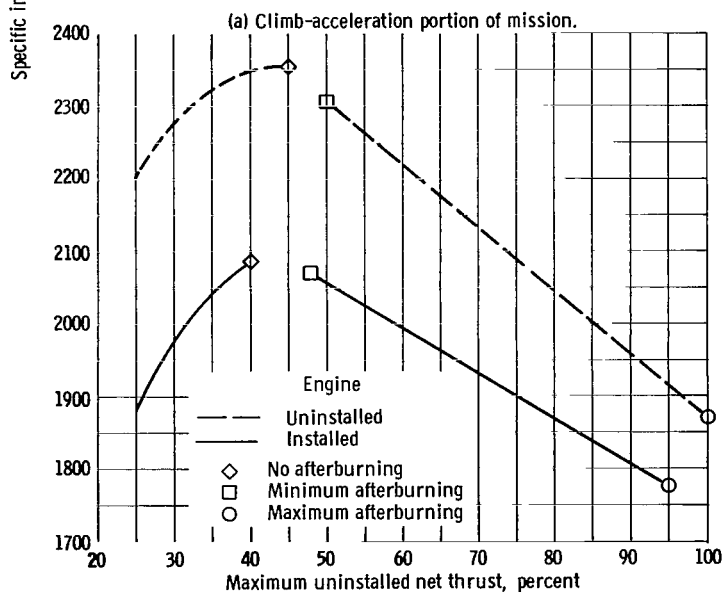
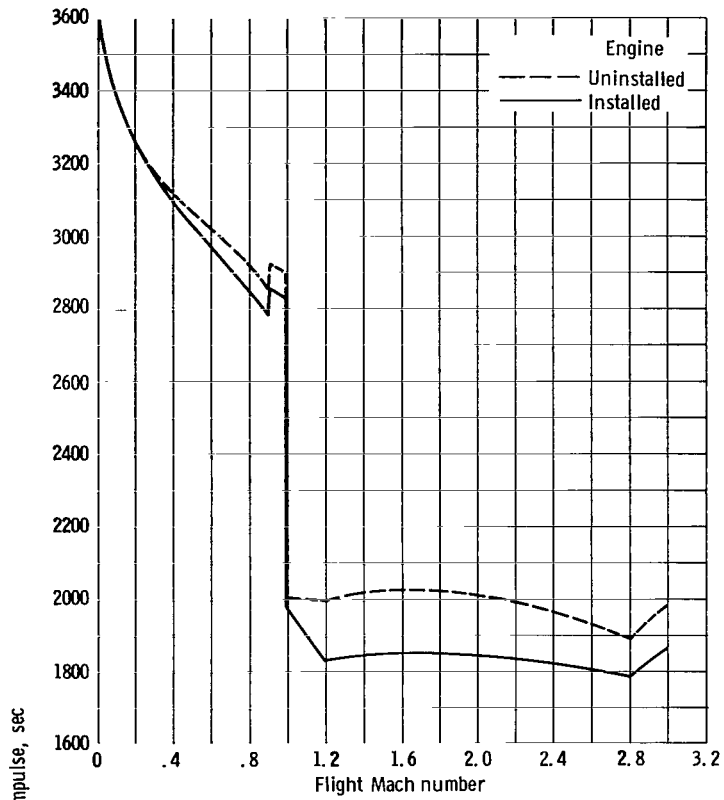
which results in a lower local Mach number. The inlet performance parameters of this analysis are based on free-stream flight Mach numbers. When the data of this report are used to evaluate inlets with performance parameters based on local Mach numbers less than free stream, these parameters must be referred to free-stream flight Mach numbers before the effect of inlet performance perturbations on the payload is determined.

The linear variations of the drag coefficients with flight Mach number closely resemble the actual variation of the individually calculated drag coefficients, which are shown in the appendix. The drag coefficients include excess-flow (a combination of oblique shock or bypass spillage), boundary-layer-bleed, cowl-lip and nacelle-wave, and nacelle-skin-friction drag coefficients. The total-inlet-nacelle installation drag coefficient (also shown in fig. 7) is obtained by adding the drag coefficients after they have been referred to a common reference capture area  $A_c$ . Each inlet performance parameter was varied independently, which is not normally the case but such an assumption was necessary for this study.

## Installed Engine Performance

Installation of the turbojet into an inlet-nacelle combination has a significant effect on the engine performance when the inlet-nacelle installation drag is accounted for as a reduction in engine performance. Figure 8 shows installed and uninstalled performance of the afterburning turbojet. The installed engine performance is that which includes the thrust degradation resulting from the inlet-nacelle installation drag, while the uninstalled performance includes only the reference-inlet-pressure recovery and the actual nozzle. Figure 8(b) presents the specific impulse for the mode of operation that is used during takeoff, climb-acceleration. The engines are operating in the manner previously described. The effect of installation drag with Mach number on engine specific impulse can be seen. At flight Mach 1.2, an 8-percent specific-impulse decrease results, while at Mach 2.8, a 6-percent specific-impulse decrease from the installation drag results. The decreasing effect of installation drag with increasing Mach number results from the change of excess-flow drag with Mach number.

At Mach 3 cruise, the afterburner temperature is reduced below the level used for climb. The part-power Mach 3 cruise engine specific impulse as a function of net thrust is shown in figure 8(b). The decrease in specific impulse due to the engine installation drag varies with thrust setting: it is 15 percent lower at the lowest power setting and 5 percent lower at the highest thrust setting. The peak specific impulse occurs without afterburning at the design-turbine-inlet temperature of  $2100^{\circ}$  F. Points to the left of the peak represent conditions of lower, off-design, turbine-inlet temperatures, still without afterburning. Points to the right of the peaks, going from left to right, represent condi-



(a) Climb-acceleration portion of mission.

(b) Cruise portion of mission.

Figure 8. - Effect of installation drag on specific impulse. Afterburning turbojet engine maximum turbine inlet temperature, 2100° F.

tions of maximum design-turbine-inlet temperature with increasing afterburner temperatures.

## Engine and Airframe Sizing

Before it can be assumed that the engine and wing sizes, which maximize payload, produce the optimum airplane, certain performance criteria must be investigated. Reference 4 indicates that a wing loading of 73 pounds per square foot and a takeoff thrust to weight ratio of 0.26 maximize the number of passengers. However, certain performance criteria were not met when this optimum wing loading and engine size were used. Among these criteria are such parameters as lift-off distance and velocity as well as transonic acceleration. Because of these factors, the design airplane for this study was selected with a takeoff wing loading of 54.7 pounds per square foot and a takeoff thrust to weight ratio of 0.32 with a resulting payload of 208 passengers. These takeoff criteria require a wing area of 8800 square feet and a sea-level static design-engine corrected airflow of 490 pounds per second, both of which will remain fixed for the remainder of this report.

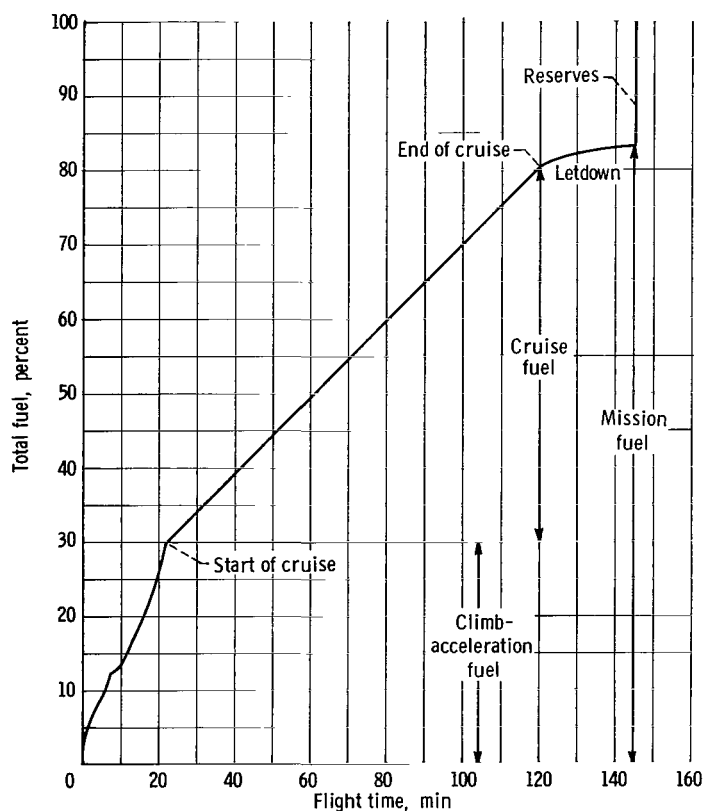


Figure 9. - Total fuel utilization schedule for reference mission. Total fuel, 216 926 pounds.

For this particular design, the lift-off distance on a standard day would be 4350 feet with a corresponding lift-off velocity of approximately 165 knots.

No firm minimum transonic thrust-drag  $F/D$  requirement exists today, but many authorities believe it should be at least 1.4 on a standard day. The engine and wing combination used in this study results in a minimum transonic thrust-drag ratio of 1.9.

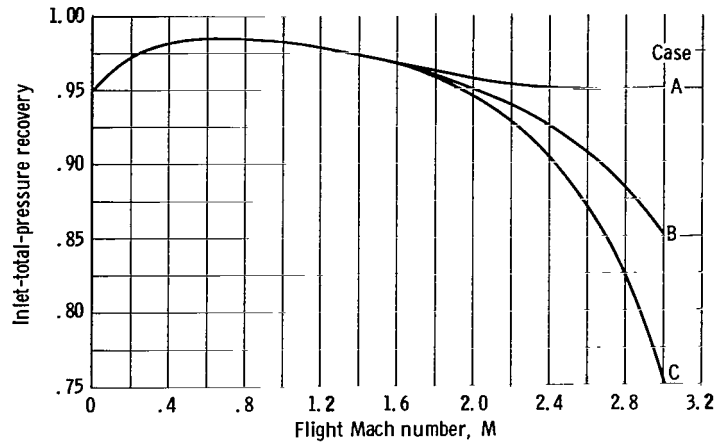
The fuel used for the mission is a function of fuel flow rate and time. The maximum fuel flow rate occurs during the climb-acceleration portion of the mission when the turbojet engine is operating in a maximum afterburning mode. This, however, is only for a short time. At cruise, even though the time is much greater, the fuel flow rate is less. Since the change in payload stems mainly from a change in mission fuel requirements, figure 9 shows the fuel utilization schedule against mission time for the reference mission shown in figure 1 (p. 4). Approximately 30 percent of the total fuel is used during the climb-acceleration to the Mach 3 cruise condition, while 51 percent is used during the cruise portion of the mission. Only 3 percent is used for letdown, and the remaining 16 percent is allocated for reserves. Thus, the inlet parameters that affect the inlet performance during cruise will probably have a greater effect on payload than will inlet parameters that are considered during the climb-acceleration portion of the mission.

## RESULTS AND DISCUSSION

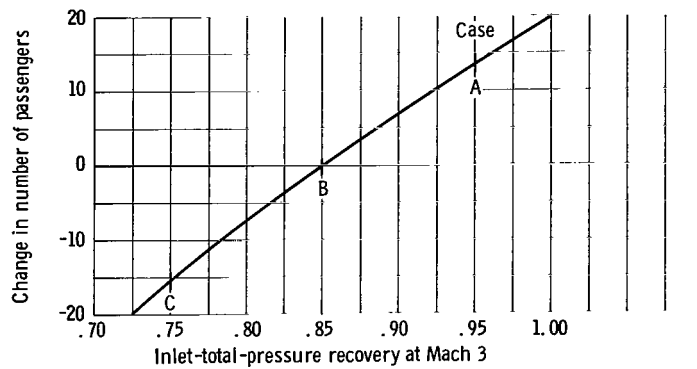
Each of the inlet-nacelle performance parameters is considered separately to determine the effect on the aircraft payload that is considered to be the important criterion for comparison. Based on the input of this study, a payload of 208 passengers for the reference inlet-nacelle, engine, and airframe combination results. The payload-carrying capability of a fixed-ramp, gross-weight aircraft is an indication of the possible returns that can be realized by the airlines. The inlet parameters that were studied are considered to cover the range of interest for the supersonic transport.

### Inlet-Total-Pressure Recovery

The inlet-total-pressure recovery was varied from 0.75 to 0.95 at cruise and varied with flight Mach number, as shown in figure 10(a). Inlet-total-pressure recovery will vary with inlet type. A low recovery in the supersonic range can result from an all-external-compression inlet: a higher recovery is obtained from the internal-compression inlet. Also, inlet-total-pressure-recovery variations can result from an attempt to increase the inlet flow stability margins by using some internal compression. These inlets can be operated with the normal shock positioned downstream of the throat.



(a) Effect of Mach number.



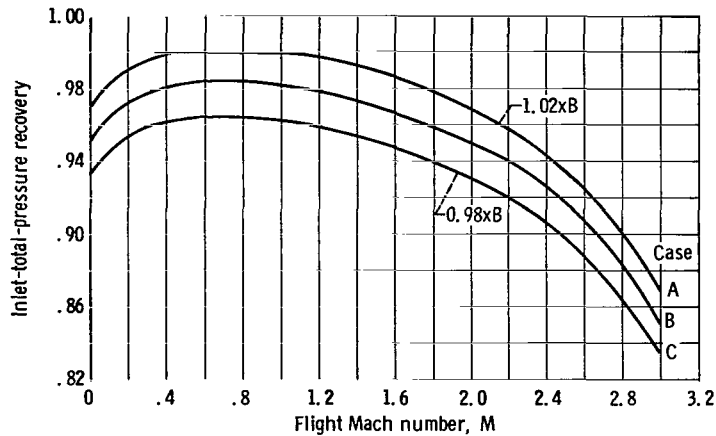
(b) Effect of inlet-total-pressure recovery on number of passengers.

Figure 10. - Inlet-total-pressure recovery.

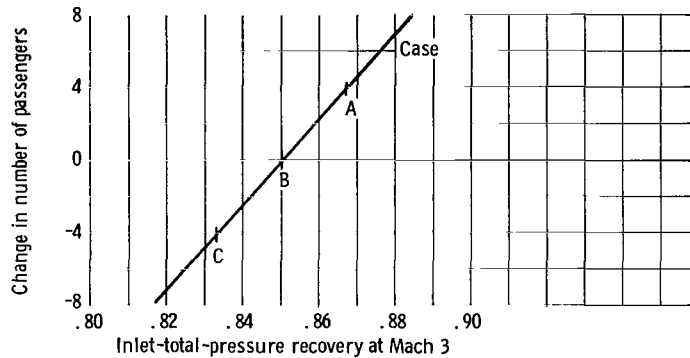
At this point, a higher Mach number exists where the normal shock occurs, thus a greater total-pressure loss will result at supersonic flight speeds. The parametric performance curves are designated as A, B, and C (fig. 10(a)), where A is considered the most optimistic, B is the reference case, and C is the most pessimistic case (unless otherwise noted).

Figure 10(b) shows that a payload decrease of 16 passengers resulted when the inlet-total-pressure recovery was decreased to 0.75 from a reference value of 0.85 at Mach 3. The points presented in figure 10(b) are for Mach 3 cruise only, but the pressure recovery of the inlets during the mission followed the schedule as a function of Mach number, as shown in figure 10(a).

An alternate means of perturbing the inlet-total-pressure recovery is shown in figure 11(a), where the reference schedule is multiplied by a factor of 0.98 and 1.02 over the entire Mach number range. A change of pressure recovery of this nature could result from differences in designing boundary-layer-bleed systems, the struts that support the spike, subsonic diffuser passage, vortex generators, or different angles on the spike



(a) Effect of Mach number.



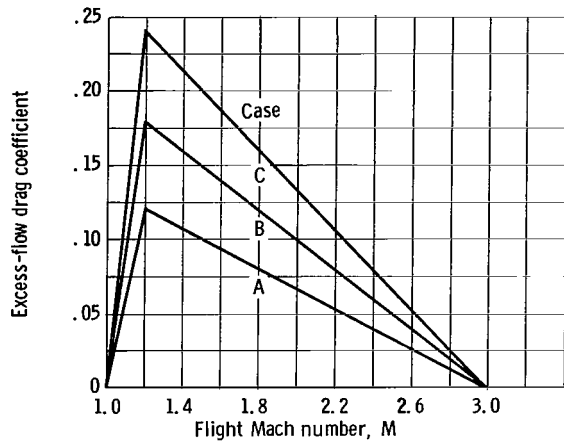
(b) Effect of inlet-total-pressure recovery on number of passengers.

Figure 11. - Inlet-total-pressure recovery.

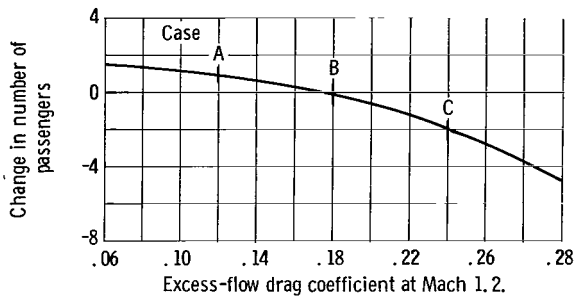
and lip, or, no doubt, many other things. This decrease in recovery of 2 percent over the entire Mach number range results in a passenger decrease of 4, as shown in figure 11(b).

### Excess-Flow Drag

The excess-flow drag is the sum of spillage airflow by either the oblique-shock or the bypass method. The oblique-shock method has the primary oblique shock detached from the inlet lip during off-design operation. The excess airflow, having passed through the oblique shock, spills around the inlet nacelle while still at supersonic velocity. However, oblique-shock spillage may require excessive spike translation distance to accomplish the required spillage, thus increasing inlet length and weight. In the bypass method, the air is accepted into the inlet, diffused to subsonic conditions in the inlet, and then bypassed through ducts to the free stream in the vicinity of the compressor face. Large ducts are required to bypass the air, thus, increasing inlet size and weight.



(a) Effect of Mach number.



(b) Effect of excess-flow drag on number of passengers.

Figure 12. - Excess-flow drag coefficient based on inlet capture area, combination of additive and bypass drag coefficient.

The excess-flow drag coefficient that may be a combination of both methods was changed from a maximum of 0.24 to a minimum of 0.12 at the transonic Mach number of 1.2 and varied with Mach number, as shown in figure 12(a). An increase of 0.06 in the excess-flow coefficient at Mach 1.2 as shown on curve C (fig. 12(a)) resulted in a payload decrease of two passengers (fig. 12(b)).

Because the flight time during the climb acceleration portion of the mission from Mach 1 to 3 was short (12 min) and minimum transonic thrust-drag  $(F/D)_{\min}$  was still high (1.87), the fuel consumed increased by 1234 pounds when the transonic drag coefficient was increased by 0.06. To fly the 3500 nautical mile mission, the aircraft used more fuel and range to climb to the optimum cruise altitude, thus it weighs less and cruises a shorter distance than the aircraft with the reference inlet. Since the total range of the mission is fixed, the cruise fuel requirement is decreased by 556 pounds. Therefore, the net fuel increase for the mission is 678 pounds, thus reducing the payload by two passengers. It should be noted that approximately 11 minutes of off-design operation are encountered during descent, but, as opposed to the high-fuel-flow rate during

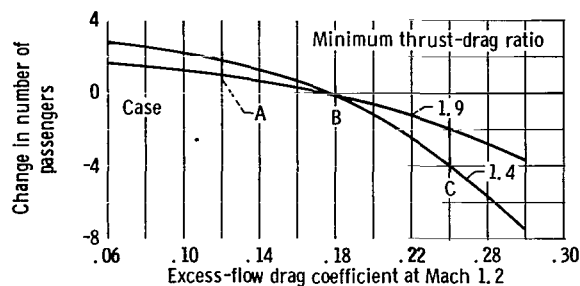


Figure 13. - Effect of transonic minimum thrust-drag ratio and excess-flow drag on number of passengers.

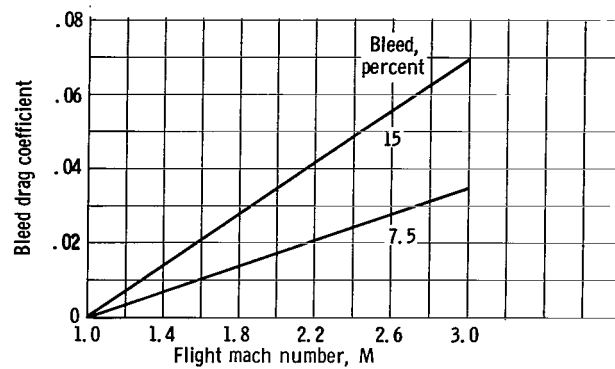
climb-acceleration, the descent fuel flow is very low and these changes are considered negligible.

All the supersonic transport configurations that will be considered probably will not have the high transonic thrust-drag margin of the SCAT 15F. If a configuration were designed that would decrease this margin to the minimum suggested value of 1.4, the effect of increasing the spillage drag coefficient by 0.06 would decrease the payload by four passengers, as shown in figure 13. Even though the effect on payload is twice the effect of the original configuration considered, the overall change in payload is still small.

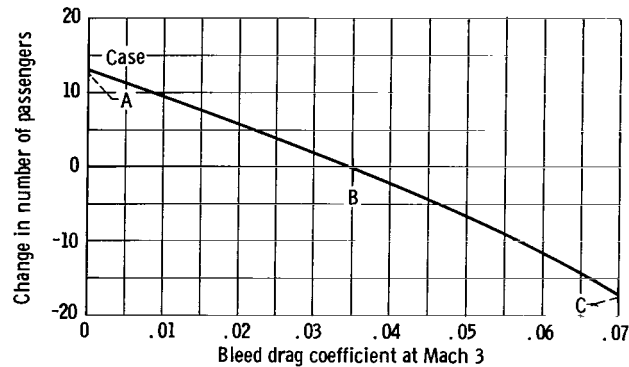
### Boundary-Layer-Bleed Drag

The drag of the boundary-layer system is based on the total momentum change and can vary considerably depending on the location and method of boundary-layer-bleed removal and the method used to discharge the bleed air into the free stream. Boundary-layer-bleed air removed prior to the normal shock will have more momentum than will air removed after the normal shock. Also affecting the boundary-layer-air momentum is the method used to remove the air, that is, a scoop or perforation. Of great importance to the drag of the system is whether the bleed air is discharged axially, or inclined with regard to the free stream, or whether the discharge nozzle is sonic or fully expanded. A change in any of these conditions will affect the drag.

The reference inlet has a boundary-layer-bleed drag coefficient of 0.035 at Mach 3. This coefficient corresponds to bleeding 7.5 percent of the inlet airflow at the conditions described in the appendix. The bleed of inlet airflow was varied from 0 to 15 percent, which corresponds to an estimated variation in boundary-layer-bleed drag coefficient from 0 to 0.070 at Mach 3 cruise (fig. 14(a)). When the coefficient was increased from the reference case B by 0.035 at Mach 3 (case C), which corresponds to a 7.5-percent bleed-flow increase, a decrease of 17 passengers resulted (fig. 14(b)).



(a) Effect of mach number.



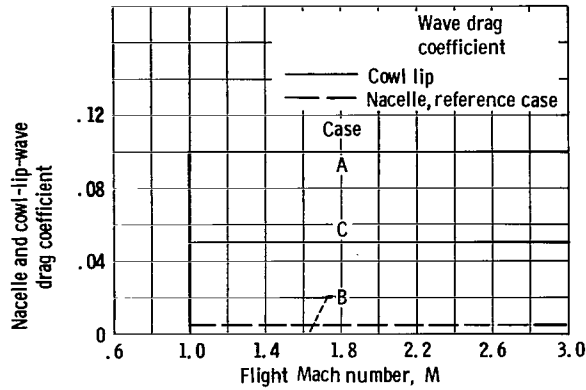
(b) Effect of bleed drag on number of passengers.

Figure 14. - Bleed drag coefficient based on inlet capture area.

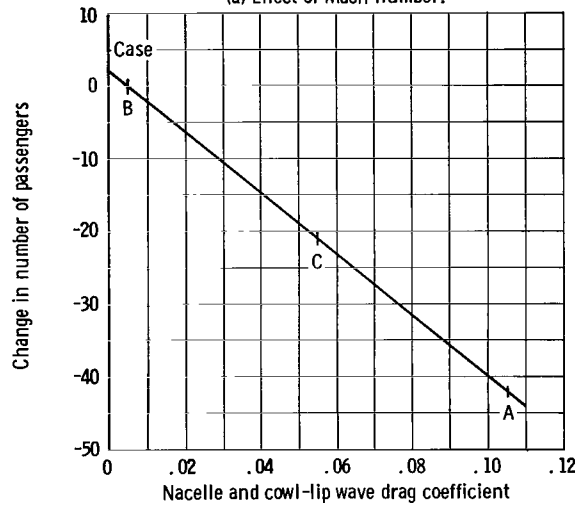
## Cowl-Lip and Nacelle-Wave Drag

The cowl-lip and nacelle-wave drag are affected by changes in inlet and nacelle geometry. It is recognized that, when a highly integrated airframe and propulsion system such as the SCAT 15F is considered, changing inlet-nacelle shapes could result in changes in the shock pattern that act on the external surfaces. These changes could be reflected in the airplane aerodynamics by a change in interference drag. However, these effects are outside the scope of this analysis. For simplicity, the calculations consider the wave drag coefficient of the inlet-nacelle combination as if it were an isolated nacelle (constant interference effects). However, this could also be interpreted for an integrated airplane as an overall change in airplane drag coefficient reflecting favorable or unfavorable inlet-nacelle interference drag that results from changes in nacelle geometry.

The reference inlet was assumed to have no cowl-lip-wave drag and a 0.005 nacelle-wave drag, which was held constant (fig. 15(a)). The variation of the cowl-lip-wave drag was assumed to have characteristics similar to the nacelle-wave drag. The wave drag which can be considered as an increase in either cowl-lip or nacelle-wave drag was



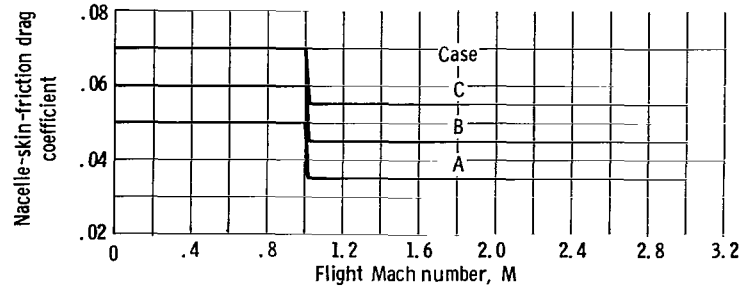
(a) Effect of Mach number.



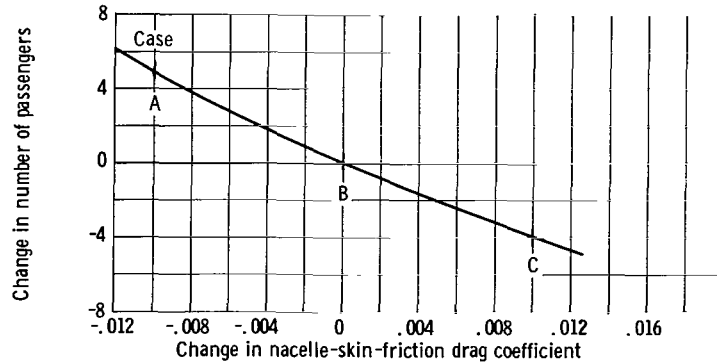
(b) Effect of nacelle and cowl-lip-wave drag on number of passengers.

Figure 15. - Nacelle and cowl-lip-wave drag coefficient, based on inlet capture area.

varied from 0 to 0.10 at the supersonic speeds, as shown in figure 15(a). Figure 15(b) shows the large effect on the number of passengers. A 0.05 increase in the cowl-lip or nacelle-wave drag coefficient decreased the number of passengers by 21. The 21-passenger decrease corresponds to an added need for 6751 pounds of fuel to complete the mission (2078 lb from the climb-acceleration phase and 4673 lb from the cruise phase). As shown in figure 10 (p. 13), the cruise portion of the flight time is the longest and approximately 61 percent of the mission fuel is used during this period. Therefore, it should be noted that any compromise which affects the inlet performance during cruise should be carefully investigated.



(a) Effect of Mach number.



(b) Effect of nacelle-skin-friction drag on number of passengers.

Figure 16. - Nacelle-skin-friction drag coefficient, based on inlet capture area.

## Nacelle-Skin-Friction Drag

Nacelle-skin-friction drag is related to inlet-nacelle geometry. The length of the inlet is dependent on the method used to compress and diffuse the supersonic flowstream. A longer inlet is required if an all-internal-compression inlet is used. A longer inlet has a greater wetted surface area and, consequently, the skin-friction drag increases. An all-external-compression inlet has minimum length, and, conversely, skin-friction drag decreases.

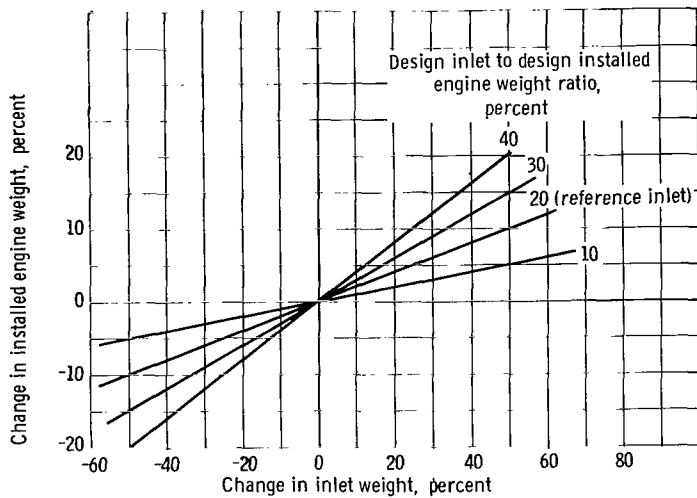
The skin-friction drag coefficient based on the reference-inlet capture area was perturbed  $\pm 0.01$  over the flight Mach number range (fig. 16(a)). An increase of 0.01 in drag coefficient resulted in a passenger decrease of 4, as indicated in figure 16(b).

A total surface-area increase of 25 percent only increases the skin-friction coefficient by 0.012 when the coefficient is referred to the inlet capture area  $A_c$ . If the entire surface-area increase is a result of an addition to the inlet surface area only and  $A_c$  remains the same, an inlet length 60 percent greater than the reference inlet is required. This significant inlet-length increase would decrease the payload by five passengers because of the increased skin-friction drag.

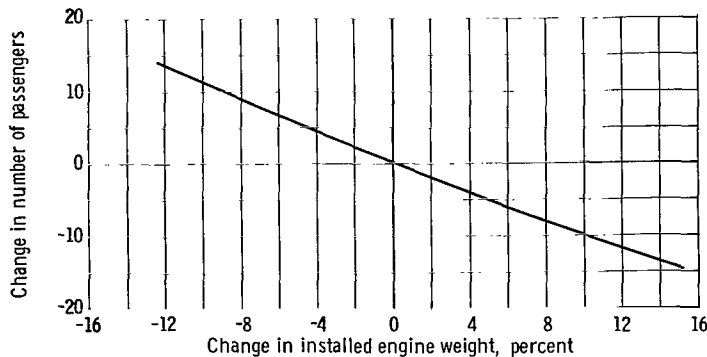
## Inlet Weight

The type of inlet and degree of variable geometry are two of many factors that affect the inlet weight. The inlet weight is included as part of the total installed engine weight that also includes nacelle, gas generator, and nozzle and reverser weights.

Figure 17(a) shows the effect of inlet-weight changes on the overall installed engine weight for various design-inlet to installed-engine weight ratios. For example, the total installed reference engine weight is 11 500 pounds per engine, and the reference inlet weight is 2300 pounds, hence, the ratio of design inlet to (installed) engine weight is 20 percent. With a design-inlet to installed-engine weight ratio of 20 percent, a 20-percent increase in inlet weight increases the installed engine weight by 4 percent (fig. 17(a)). A 4-percent increase in installed engine weight will decrease the payload by four passengers (fig. 17(b)). However, if the ratio of inlet to installed-engine weight were 40 percent, a 20-percent change in inlet weight would increase the installed engine weight



(a) Effect of inlet weight on installed engine weight.



(b) Effect of installed engine weight on number of passengers.

Figure 17. - Inlet weight.

by 8.0 percent (fig. 17(a)), and a decrease of approximately eight passengers would result (fig. 17(b)).

### Summary of Effects of Inlet Perturbations on Payload

Table I summarizes the effect on payload of perturbing the values of inlet parameters of the reference inlet (case B) to the inlet parameters represented by case C for an airplane similar to the SCAT 15F configuration cruising at Mach 3. Consideration of the lower bound inlet parameters (i.e., incremental changes from case B to C) showed that cowl-lip and nacelle-wave drag, boundary-layer-bleed drag, and inlet-total-pressure recovery had a greater effect on payload than did inlet weight, skin-friction drag, and transonic excess-flow drag.

To this point, only a Mach 3 cruise SCAT 15F configuration has been considered. To determine the effect of the inlet parameter perturbations on payload during cruise at a lower Mach number, the SCAT 15F airframe, engines, and inlets were redesigned to cruise at Mach 2.7. The drag characteristics were varied with Mach number, as shown in figure 18. Illustrated in this figure is the reference inlet case B. The same magnitude of variations of cases A and C of the inlet parameters at Mach 2.7 cruise was investigated

TABLE I. - EFFECT OF INLET DEGRADATION ON PASSENGER  
LOAD OF SCAT 15F POWERED BY FOUR 2100° F  
AFTERBURNING TURBOJET ENGINES  
[Reference number of passengers, 208.]

Perturbation	Cruise	
	Mach 3	Mach 2.7
	Decrease in number of passengers	
Increase of 0.05 in cowl-lip or nacelle-wave drag coefficient	21	25
Increase of 7.5 percent inlet flow in cruise bleed flow	17	19
Drop of 0.10 in cruise inlet-total-pressure recovery	16	26
Increase of 20 percent in inlet weight if $\frac{\text{Design inlet weight}}{\text{Design installed engine weight}} = 20 \text{ percent}$	4	4
Increase of 0.01 in skin-friction drag coefficient	4	5
Increase of 0.06 in transonic excess-flow drag coefficient	2	2

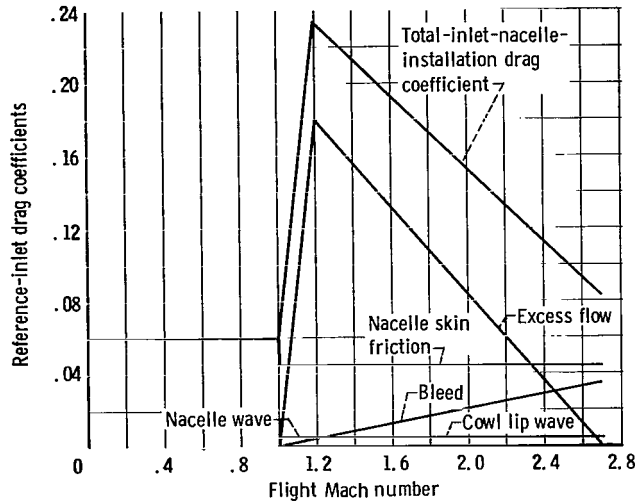


Figure 18. - Drag characteristics of reference inlet based on inlet capture area at Mach 2.7. Total drag coefficient equal to excess flow plus nacelle friction plus nacelle wave plus cowl lip wave plus bleed drag coefficients.

as was done for the Mach 3 cruise. The results of incremental changes from case B to C are shown in table I. It is indicated that cruise inlet performance has greater effect on payload at Mach 2.7 than at Mach 3 cruise. In general, however, characteristics of the payload against inlet parameters do not change when the cruise Mach number is decreased to 2.7.

### Comparison of Several Inlet Types

Five different inlets were used to illustrate whether an inlet, possibly with a higher pressure recovery but with more external drag, will enable the airplane to have a higher payload capability than will an inlet with a decrease in pressure recovery, drag, and possibly less weight. The inlets used as examples and schematically shown in figure 19 are generally classified into five groups depending where the supersonic diffusion takes place. The inlets used were (1) external compression, (2) low-drag external compression, (3) self-start external plus internal compression, (4) external plus internal compression, and (5) internal compression. These inlets have, for the sample comparison, the approximate performance and weight characteristics, as shown in table II, in order to illustrate the use of the parametric curves to determine how changes in inlet performance and weight affect payload. The effect of the inlet-parameter perturbations from the reference inlet are expressed as a payload increment or decrement. When more than one inlet parameter is varied, the payload changes are added algebraically to the 208 passenger reference payload. The effect of the inlet perturbations are shown in table III.

TABLE II. - SAMPLE COMPARISON OF INLET TYPES

Heading	Inlet					
	Refer- ence	External	Low-drag external	Self-start mixed	Mixed	Internal
Pressure recovery at Mach 3	0.85	0.80	0.80	0.86	0.86	0.91
Change in pressure recovery from reference	0	-.05	-.05	.01	.01	.06
Excess-flow drag coefficient at Mach 1.2	.18	.06	.06	.12	.12	.250
Change in excess-flow drag coefficient	0	-.12	-.12	-.06	-.06	.07
Bleed flow, percent of inlet airflow at Mach 3	7	4	7	8	10	15
Bleed drag coefficient at Mach 3	.035	.018	.035	.038	.047	.070
Change in bleed drag coeffi- cient	0	-.017	0	.003	.012	.035
Cowl-lip external angle, deg	0	28	22	4	0	0
Cowl-lip-wave drag coeffi- cient at Mach 3	0	.10	.05	.01	0	0
Change in cowl-lip-wave drag coefficient	0	.10	.05	.01	0	0
Nacelle-wave drag coefficient at Mach 3	.005	.0250	.010	.005	.004	0
Change in nacelle-inlet-wave drag coefficient	0	.020	.005	0	-.001	-.005
Nacelle-inlet skin-friction drag coefficient at Mach 3	.045	.043	.045	.045	.048	.055
Change in nacelle-inlet skin- friction drag coefficient	0	-.002	0	0	.003	.010
Relative inlet weight	100	.65	.65	.83	1.10	1.35
Change in inlet weight	0	-.35	-.35	-.17	.10	.35

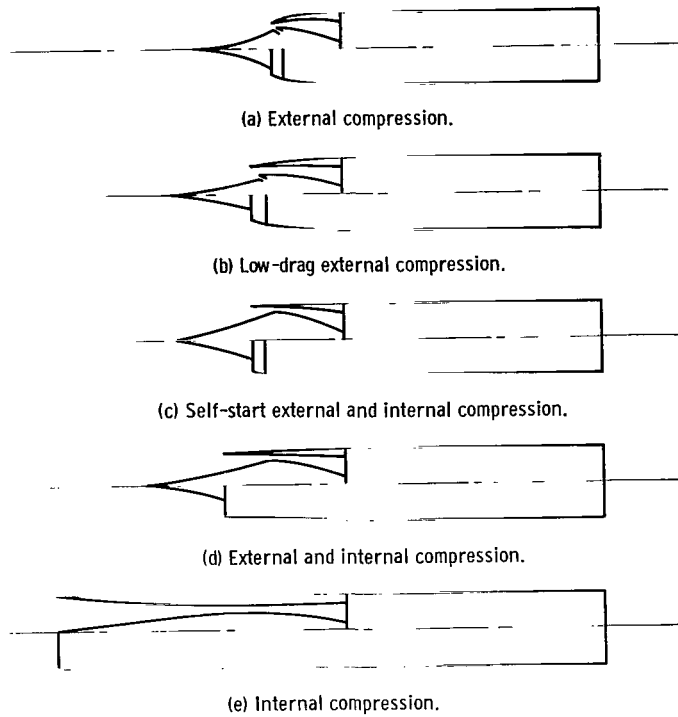


Figure 19. - Inlet compression systems.

TABLE III. - INCREMENTS IN PASSENGERS AT MACH 3 CRUISE  
REFERENCE PAYLOAD OF 208 PASSENGERS

Effect on number of passengers due to -	Inlet						
	Refer- ence	External	Low-drag external	Self-start mixed	Mixed	Internal	Figure
Inlet-total-pressure recovery	0	-7.0	-7.0	1.9	1.9	8.7	11
Excess-flow drag coefficient		1.6	1.6	1.0	1.0	-2.4	13
Bleed drag coefficient		6.5	0	-1.3	-5.2	-17.0	15
Cowl-lip-wave drag coefficient		-42.0	-21.3	-4.3	0	0	16
Nacelle-inlet-wave drag coefficient		-8.5	-2.0	0	.3	2.0	16
Nacelle-inlet skin-friction coefficient		1.0	0	0	-1.2	-4.0	17
Inlet weight		7.5	7.5	3.7	-2.0	-7.0	18
Total change in number of passengers		-40.9	-21.2	1.0	-5.2	-19.7	
Relative number of passengers	1.000	.803	.898	1.005	.975	.905	

A comparison of the five general inlets is used to illustrate the use of the curves by assuming general performance characteristics for each inlet. This comparison shows that the self-starting mixed-compression inlet provided the greatest aircraft payload capability when installed on the afterburning turbojet engine. The performance assumed for the all-external-compression inlet provided the lowest payload capability, while the other inlets, including the all-internal-compression inlet were between the self-starting-mixed and external-compression inlets when payload only was considered. The inlet that yields the maximum payload is important when only the economic aspects of the aircraft are considered; however, it is not necessarily the one to select. There are qualitative factors such as stability, complexity and reliability, self-starting, controllability, sensitivity to angle of attack, etc. The compromise in inlet performance and weight have to consider both the qualitative and economic factors involved.

## CONCLUDING REMARKS

An analytical study was made to provide a means of evaluating various inlet designs on a fixed arrow-wing transport configuration. The curves presented permit inlets of different design to be evaluated in terms of design passenger carrying capacity. Examples have been presented that illustrate the use of the curves. Various characteristics for different inlet designs were assumed. The payload capability of the transport cruising at Mach 3 was compared.

The inlet parameters investigated showed that aircraft performance was most sensitive to cowl-lip and nacelle-wave drag, boundary-layer-bleed drag, and inlet-total-pressure recovery, but less sensitive to inlet weight, skin-friction drag, and transonic excess-flow drag. A decrease in design cruise Mach number from 3 to 2.7 did not change the general characteristics of the curves of inlet parameters as a function of payload; however, the cruise inlet performance has greater effect on payload during cruise at Mach 2.7 than at Mach 3.

The results are probably most useful for comparison of inlets when considering aircraft with similar performance, weight, engine type, and configuration as the one used in this analysis. Similar trends, however, would be expected for other airframes and/or engines when the curves are used to approximate payload changes that result from inlet performance and weight trade-offs.

Lewis Research Center,  
National Aeronautics and Space Administration,  
Cleveland, Ohio, October 19, 1966,  
126-15-02-02-22.

## APPENDIX - CALCULATION OF INLET-NACELLE DRAG COEFFICIENTS

The approximate values of the reference-inlet and nacelle drag coefficients were calculated by analytical methods with the inlet-total-pressure recovery and engine-airflow schedules shown in figures 5 (p. 7) and 6 (p. 8), respectively. The analytical methods of predicting the variation of the drag coefficients as a function of Mach number and inlet and nacelle geometry have been substantiated by actual test data in the references 6 to 10. Each inlet drag coefficient was calculated separately, referred to a common reference area, and added to give the total installation drag coefficient.

### Excess-Flow Drag

The axisymmetric mixed-compression reference inlet was sized to capture the entire free-stream tube at the Mach 3 cruise condition. At Mach numbers less than cruise, the excess airflow is spilled by a combination of oblique shock and bypass spillage. The oblique-shock-spillage airflow is limited by the maximum spike translation that, for this inlet, resulted in a cowl position parameter of  $22^\circ$ . This limit necessitated the spillage of some airflow through a bypass system that used a sonic nozzle discharge at a  $15^\circ$  angle relative to the free stream to reenter the airflow to the free stream. Figures 20 and 21,

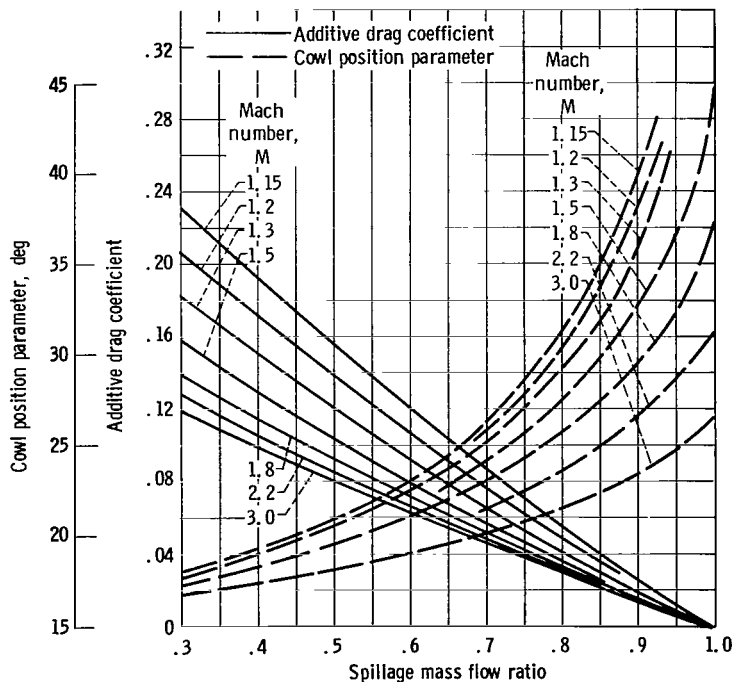


Figure 20. - Additive-drag coefficient, based on inlet design capture area. Cone half angle,  $15^\circ$ .

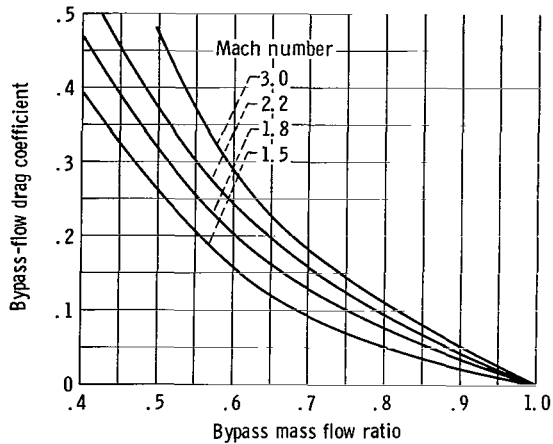


Figure 21. - Bypass flow drag coefficient, based on inlet capture area; exit, sonic nozzle.

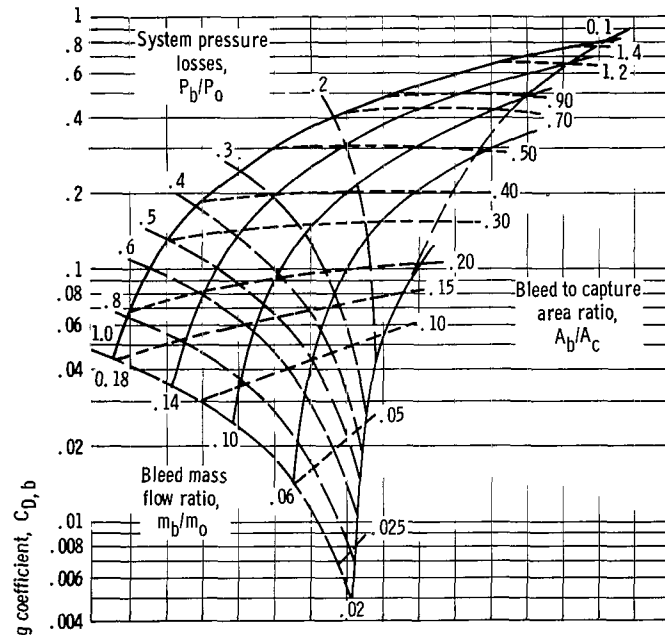
taken from references 6 and 7, respectively, were used to calculate the total excess-flow drag coefficient when the required engine-airflow schedule during off-design operating condition is as shown in figure 6 (p. 7). The excess-flow drag coefficient as a function of Mach number based on an inlet capture area  $A_c$  is shown on figure 26.

### Boundary-Layer Bleed-Flow Drag

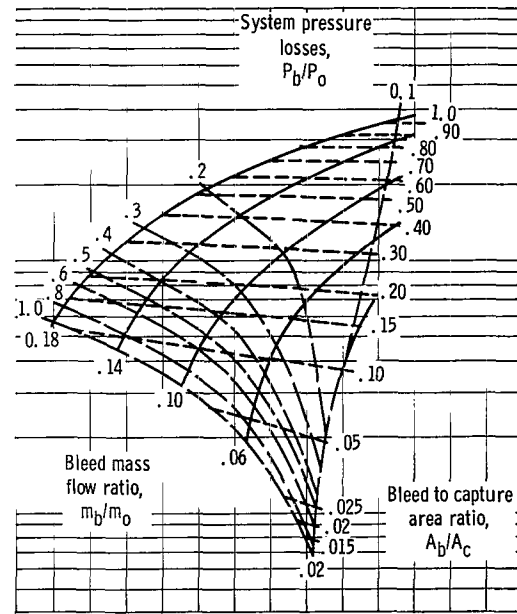
Boundary-layer bleed is usually required in all inlets in different amounts. In the mixed-compression inlet that was considered, the boundary-layer bleed was used to obtain greater flow stability and a more uniform pressure distribution at the compressor face. For the removal of the boundary-layer air, a system is required to duct air overboard through an auxiliary exit. The drag of the system was based on the total axial momentum change between the discharge station and the free stream. The discharge was assumed to be through a sonic nozzle discharging in a direction axial to the free stream.

Bleed drag coefficients were calculated for different system pressure losses  $P_b/P_o$ , bleed-mass-flow ratios  $m_b/m_o$ , bleed- to capture-area ratio  $A_b/A_c$  ( $A_b$  is the area of the bleed duct where conditions exist such that the local speed is equal to the speed of sound), and free-stream Mach numbers. The resulting boundary-layer-bleed drag coefficients are shown in figure 22 for Mach 1.5, 2.0, 2.5, and 3.0. The drag coefficients, as presented, assume a bleed-discharge exit-nozzle thrust coefficient of 0.9. If the bleed nozzle thrust coefficient were decreased, the drag penalty would be greater.

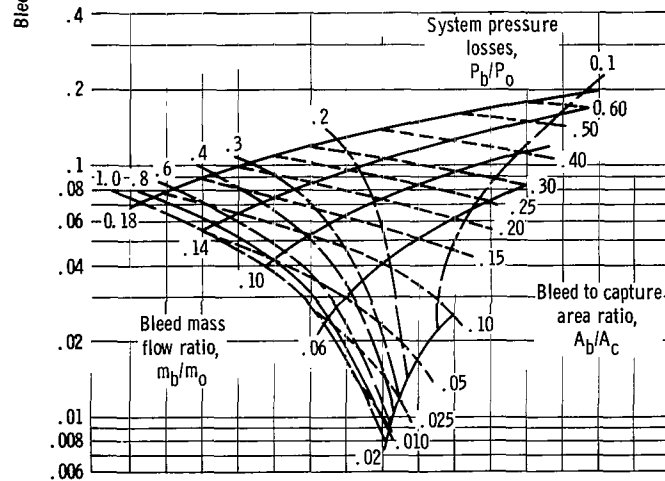
Normally, the bleed- to capture-area ratio is fixed for a certain inlet design. The parameter  $A_b/A_c$  illustrates the increase in the bleed-system-pressure recovery required to increase the bleed airflow if a variable bleed-area design is not feasible.



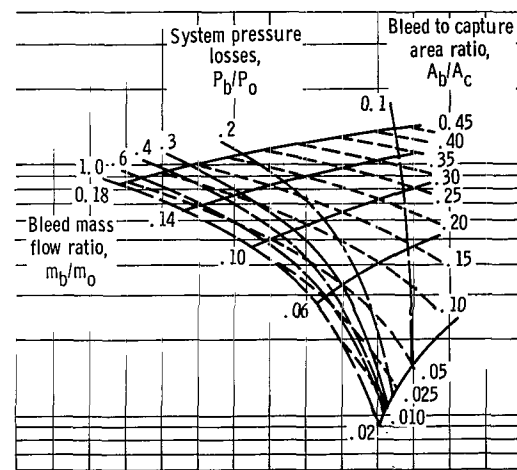
(a) Mach 1.5.



(b) Mach 2.



(c) Mach 2.5.



(d) Mach 3.0.

Figure 22. - Bleed drag coefficients.

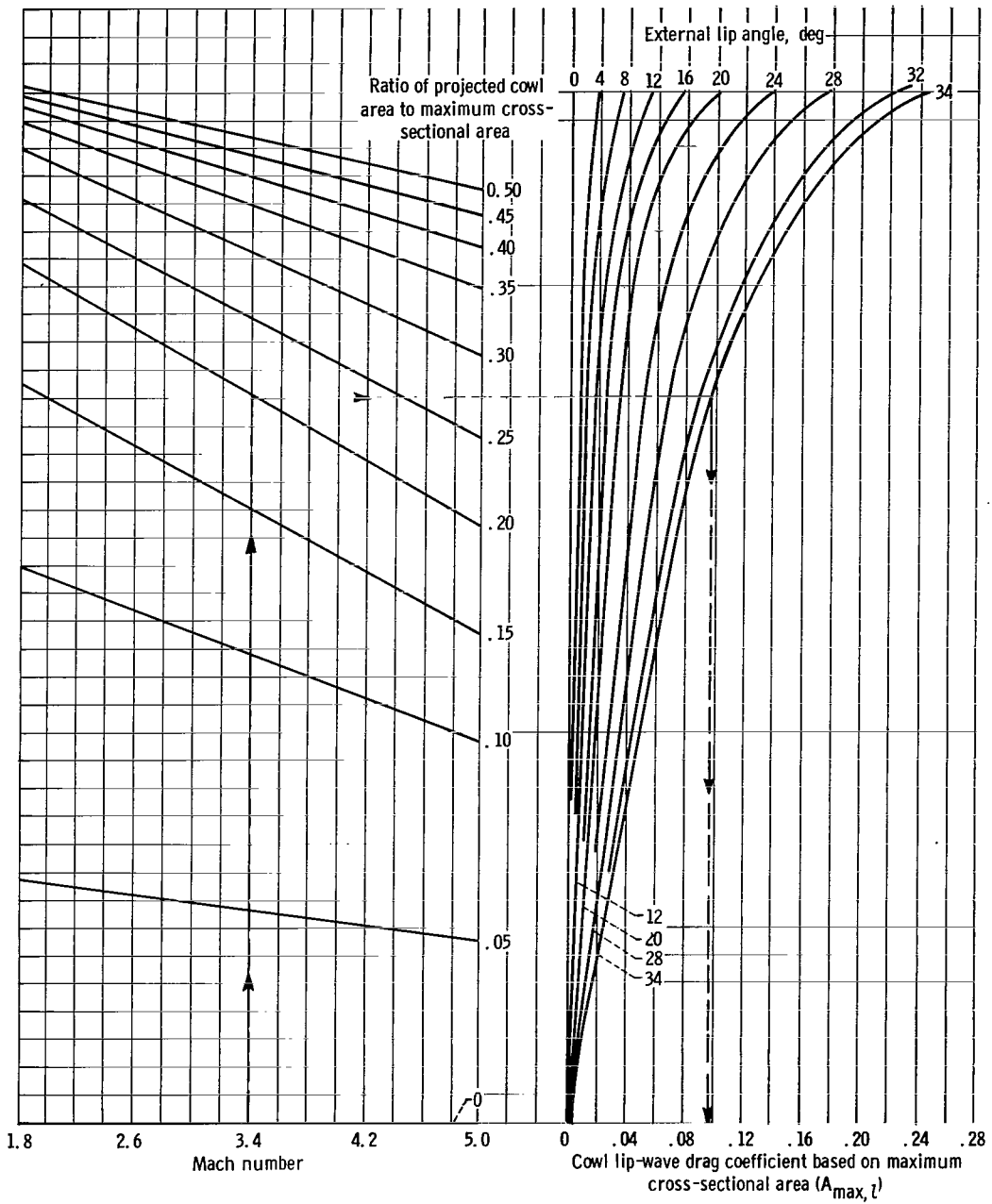


Figure 23. - Empirical chart for estimating cowl lip-wave coefficients of cowls approaching an elliptic contour (ref. 8).

For the calculation of the boundary-layer-bleed drag coefficient of the reference inlet, a bleed-airflow-mass ratio  $m_b/m_o$  of 0.075 was required at Mach 3 cruise conditions. The boundary-layer-bleed airflow decreased linearly to zero airflow at Mach 1.0. A bleed-system total-pressure-recovery ratio  $P_b/P_o$  of 0.75 and a bleed- to free-stream-area ratio  $A_b/A_o$  of 0.0275 resulted in a boundary-layer-bleed drag coefficient as a function of Mach number (fig. 26).

## Cowl-Lip and Nacelle-Wave Drag

The calculations consider the wave drag coefficient of the inlet nacelle as an isolated nacelle. It should be recognized that, when a highly integrated airframe and propulsion system such as the SCAT 15F are considered, the inlet-nacelle geometry changes could result in changes in the airplane aerodynamics by a change in interference drag. However, for simplicity, interference drag was assumed to be constant for this study.

For illustrative purposes, the cowl-lip and nacelle-wave drag coefficients were calculated as two independent parameters. For these separate wave-drag-coefficient calculations, it was assumed that the cowl lip ended 10 inches from the leading edge of the inlet lip, while the remaining length of the part where the area is changing was accounted for as nacelle-wave drag.

The reference mixed-compression inlet has some degree of external compression; therefore, the supersonic flow must be turned on the ramp side of the inlet. The degree of turning depends on the amount of external compression. To accomplish this turn, the inlet required a curved cowl lip that resulted in a pressure or wave drag when the pressure was integrated over the external surface of the changing area.

The wave drag coefficient of a cowl lip that has an elliptical contour is shown in figure 23 (from ref. 8). The initial cowl-lip angle for the inlet was  $20^\circ$  with a ratio of projected cowl area to maximum cross-sectional area of 0.0528. The cowl-lip-wave drag coefficient for different Mach numbers is shown in figure 26.

The area change in the supersonic flow field, which causes the nacelle-wave drag, is the remaining area increase from the maximum cowl-lip area to the maximum engine nacelle area, which for this analysis is the engine accessory compartment. The nacelle-wave drag coefficient for a slender conical forebody is shown in figure 24 (from ref. 9). The variation of the nacelle-wave drag coefficient for the reference nacelle-inlet combination as a function of Mach number is also shown in figure 26.

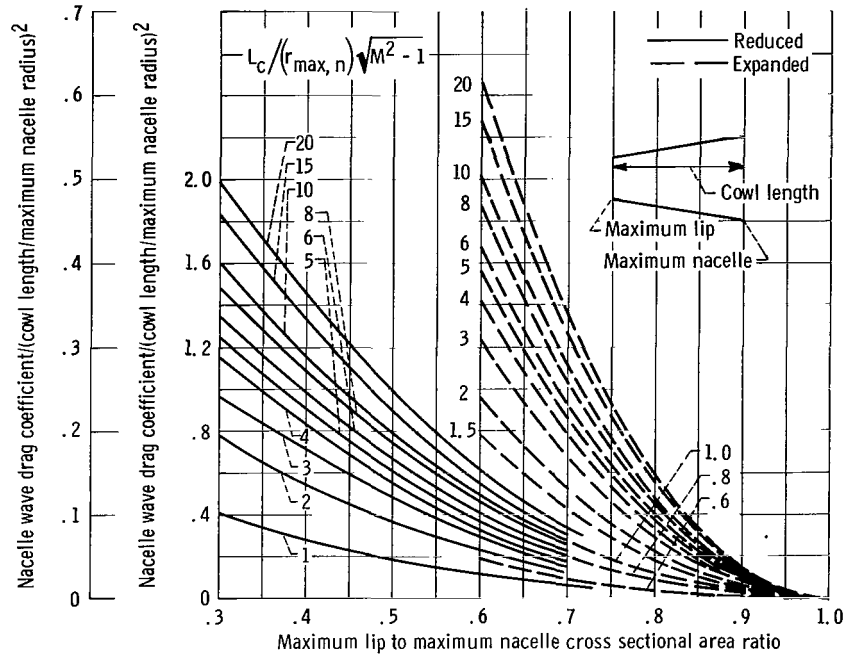


Figure 24. - Wave drag coefficient for slender conical fore or afterbodies based on maximum nacelle area,  $A_{max, N}$ ; cowl length / {maximum nacelle radius [(flight Mach number)<sup>2</sup> - 1.0]<sup>1/2</sup>},  $L_c / (r_{max, n}) \sqrt{M^2 - 1}$  (ref. 9).

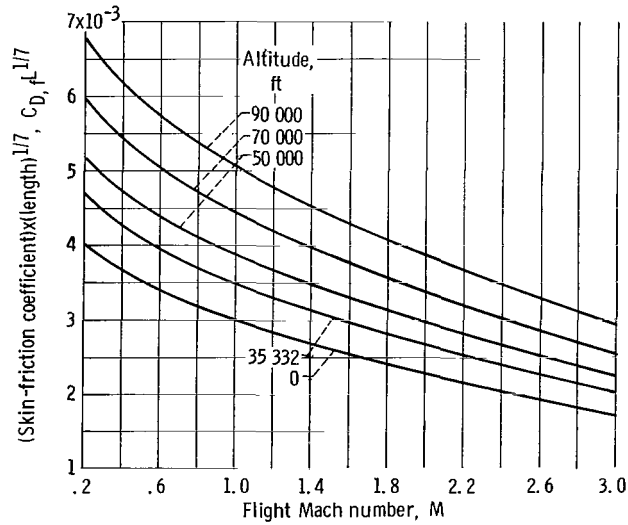


Figure 25. - Turbulent skin-friction coefficient based on wetted area (ref. 10).

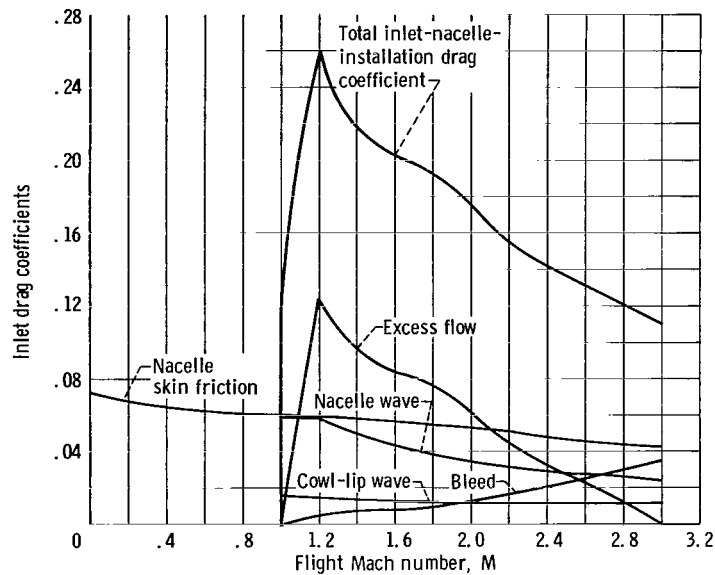


Figure 26. - Calculated drag coefficients of reference inlet, based on inlet capture area at Mach 3.

## Skin-Friction Drag

The skin-friction drag is affected by a number of factors such as laminar or turbulent boundary layer, Mach number, Reynolds number, and static-pressure gradient. Generally, the boundary layer is assumed to be turbulent and the surface smooth. The skin-friction drag coefficient for turbulent flow for several altitudes is shown in figure 25 (ref. 10). The coefficient is shown based on the square feet of total surface area. The total surface area was calculated by assuming the inlet-nacelle combination of a truncated conical forebody and a cylindrical afterbody. The corresponding skin-friction drag coefficient was referred to the inlet capture area and is shown as a function of Mach number in figure 26 for the typical flight path (see fig. 1).

## REFERENCES

1. Stroud, J. F.; and Benson, J. L.: SST Inlet Studies. Paper No. 64-597, AIAA, Aug. 10, 1964.
2. Hand, W. H.: Compatibility Considerations for a Supersonic Transport Engine Performance Specification. Paper 62-AV-29, ASME, June 1962.
3. Connors, James F.; and Allen, John L.: Survey of Supersonic Inlets for High Mach Number Applications. NACA RM E58A20, 1958.
4. Whitlow, John B., Jr.; Eisenberg, Joseph D.; and Shovlin, Michael D.: Potential of Liquid-Methane Fuel for Mach 3 Commercial Supersonic Transports. NASA TN D-3471, 1966.
5. Dugan, J. F., Jr.; Koenig, R. W.; Whitlow, J. B., Jr.; and McAuliffe, T. B.: Power for the Mach 3 SST. *Astron. Aeron.*, vol. 2, no. 9, Sept. 1964, pp. 44-53.
6. Sibulkin, Merwin: Theoretical and Experimental Investigation of Additive Drag. NACA TR 1187, 1954.
7. Hearth, Donald P.; and Connors, James F.: A Performance Analysis of Methods for Handling Excess Inlet Flow at Supersonic Speeds. NACA TN 4270, 1958.
8. Samanich, Nick E.: Pressure Drag of Axisymmetric Cowls Having Large Initial Lip Angles at Mach Numbers from 1.90 to 4.90. NASA Memo 1-10-59E, 1959.
9. Fraenkel, L. E.: The Theoretical Wave Drag of Some Bodies of Revolution. Rep. No. R&M2842, Aeronautical Research Council, 1955. (Supersedes Aero 2420, Royal Aircraft Establishment, May 1951.)
10. Tucker, Maurice: Approximate Calculation of Turbulent Boundary-Layer Development in Compressible Flow. NACA TN 2337, 1951.

*"The aeronautical and space activities of the United States shall be conducted so as to contribute . . . to the expansion of human knowledge of phenomena in the atmosphere and space. The Administration shall provide for the widest practicable and appropriate dissemination of information concerning its activities and the results thereof."*

—NATIONAL AERONAUTICS AND SPACE ACT OF 1958

## NASA SCIENTIFIC AND TECHNICAL PUBLICATIONS

**TECHNICAL REPORTS:** Scientific and technical information considered important, complete, and a lasting contribution to existing knowledge.

**TECHNICAL NOTES:** Information less broad in scope but nevertheless of importance as a contribution to existing knowledge.

**TECHNICAL MEMORANDUMS:** Information receiving limited distribution because of preliminary data, security classification, or other reasons.

**CONTRACTOR REPORTS:** Technical information generated in connection with a NASA contract or grant and released under NASA auspices.

**TECHNICAL TRANSLATIONS:** Information published in a foreign language considered to merit NASA distribution in English.

**TECHNICAL REPRINTS:** Information derived from NASA activities and initially published in the form of journal articles.

**SPECIAL PUBLICATIONS:** Information derived from or of value to NASA activities but not necessarily reporting the results of individual NASA-programmed scientific efforts. Publications include conference proceedings, monographs, data compilations, handbooks, sourcebooks, and special bibliographies.

*Details on the availability of these publications may be obtained from:*

SCIENTIFIC AND TECHNICAL INFORMATION DIVISION  
NATIONAL AERONAUTICS AND SPACE ADMINISTRATION

Washington, D.C. 20546